

First Quasi-Lagrangian in-situ Measurements of Antarctic Polar Springtime Ozone: Observed Ozone Loss Rates from the Concordiasi Long-Duration Balloon Campaign

R. Schofield^{1,2}, L. M. Avallone^{3,4}, L. E. Kalnajs³, A. Hertzog⁵, I. Wohltmann⁶, and M. Rex⁶

¹School of Earth Sciences, University of Melbourne, Melbourne, Australia

²ARC Centre of Excellence for Climate System Science, University of New South Wales, Australia

³Laboratory for Atmospheric and Space Physics, University of Colorado, Boulder, U.S.A.

⁴National Science Foundation, Washington, U.S.A.

⁵Laboratoire de Météorologie Dynamique, Palaiseau, France

⁶Alfred Wegener Institute, Potsdam, Germany

Abstract. We present ozone measurements made using state-of-the-art ultraviolet photometers onboard three long-duration stratospheric balloons launched as part of the Concordiasi campaign in austral spring 2010. Ozone loss rates calculated by matching air-parcels sampled at different times and places during the polar spring are in agreement with rates previously derived from ozonesonde measurements, for the vortex-average, ranging between 2-7 ppbv per sunlit hour or 25-110 ppbv per day. However, the geographical coverage of these long-duration stratospheric balloon platforms provides new insights into the temporal and spatial patterns of ozone loss over Antarctica. Very large ozone loss rates of up to 230 ppbv per day (16 ppbv per sunlit hour) are observed for air-masses that are down-wind of the Antarctic Peninsula and/or over the East Antarctic region. The ozone loss rate maximum downstream of the Antarctic Peninsula region is consistent with high PSC occurrence from Calipso and large ClO abundances from MLS satellite observations for September (12th-22nd) 2010, and a chemical box model simulation using JPL 2011 kinetics with full chlorine activation.

1 Introduction

Twenty six years after the signing of the Montreal protocol, widely considered the most successful international environmental policy of our time, there is evidence that stratospheric chlorine - the primary anthropogenic contributor to stratospheric ozone loss - is returning to pre-human-influence levels. In addition, the climate protection due to the reduction of chlorofluorocarbons, halons and methylbromide mandated by the Montreal protocol exceeds carbon mitigation strate-

gies to date. Despite these successes, questions about the longitudinal variations of ozone loss rates have remained unanswered because of the technological challenges of directly measuring stratospheric ozone losses in-situ.

Stratospheric ozone, and its dramatic annual losses in the Antarctic spring, have been shown to have a strong influence over the entire southern hemispheric climate (Thompson et al., 2011). The effects include the suppression in the expected warming of the Antarctic region (Thompson and Solomon, 2002) due to increasing greenhouse gas levels and a strengthening of the polar jet. Due to the significant chlorofluorocarbon and halon reductions brought about by the Montreal Protocol, polar springtime stratospheric ozone losses are expected to return to pre-1980 levels by 2050 (Bekki et al. (2011), and consequently, the role of stratospheric ozone in modulating the southern hemisphere climate will change during this time period.

Conversely, the formation of polar stratospheric clouds (PSCs), crucial in converting chlorine from reservoir species into active radicals, has been linked to tropospheric cloud systems. Kohma and Sato (2013) demonstrate that, in 2010, 33% of PSCs between 15 and 20 km were associated with the radiative cooling resulting from blocking anticyclones and clouds in the troposphere. Thus the changing climate, which affects the presence of tropospheric cloud systems, also modulates stratospheric ozone loss.

The overall chemistry of polar ozone loss process is now well understood (Dameris et al., 2014). Polar stratospheric ozone loss occurs predominantly as a result of the ClO dimer catalytic cycle that operates in the low UV conditions of the lower stratosphere (Molina and Molina, 1987; Solomon, 1999), where other radicals such as atomic oxygen are not present, with the bromine radical catalytic cycle also playing a significant, but smaller role.

Ozone loss rates in the northern hemisphere have been relatively well studied by following and matching distinct air-masses in time using many ozonesondes in intensive ‘Match’

Correspondence to: Robyn Schofield
(robyn.schofield@unimelb.edu.au)
and Linnea Avallone
(linnea.avallone@colorado.edu)

campaigns (von der Gathen et al., 1995; Rex et al., 1998, 2002). All winters cold enough to cause significant ozone losses have been studied using Match campaigns in the Arctic. In contrast, ozone loss rates in the Antarctic have been less well studied in-situ, with Match campaigns conducted in 2003-2007, finding vortex-averaged Antarctic ozone losses of 4 ± 1 ppbv per sunlit hour for 15th August to 15th September in 2002 (Frieler et al., 2006). Using satellite remote sensing matching airmasses from observations of the POAM II (Bevilacqua et al., 1997) and III (Hoppel et al., 2005) found 85 ± 15 ppbv day⁻¹ (1994-1996) and 8 ± 6 ppbv sunlit hr⁻¹ (1998-2003), respectively for the Antarctic. For the more recent time period Antarctic vortex-average of 45 ± 6 ppbv/day has been derived from the SCIAMACHY satellite observations (Sonkaew et al., 2013). Hassler et al. (2011) used ozonesonde measurements at the South Pole to derive rates of 90 ± 10 and 70 ± 10 ppbv day⁻¹ for 1991-95 and 96-2010 periods, respectively. Observations at one fixed location do not deliver rates representative of the true in-situ loss, but compare very well to vortex-average loss rates. Ozone loss rates for the total column have been derived from the ground-based Dobson/Brewer/SAOZ network [Kuttippurath et al., 2010] of 2.5 ± 0.5 DU day⁻¹ (13th August - 2nd October 2005-2009), in good agreement with SCIAMACHY, 2.0 ± 0.3 DU day⁻¹, for the same time period and OMI, 2.4 ± 0.5 DU day⁻¹, for a shorter time period (18th August - 18th September 2002-2008). While these column loss rates are not directly comparable to in situ loss rates they are provided for completeness here, as the column loss rates influence surface UV hence the biosphere and health implications of Antarctic ozone losses. We show in this paper that both the spatial and temporal variations of the ozone loss rates in the Antarctic need to be considered moving away from vortex-average loss rates view.

This paper presents for the first time ozone loss rates measured in situ onboard quasi-Lagrangian balloons and is organised as follows. The following section provides details of the measurements. The modelling section details the match analysis and ozone loss rates derived for the balloon flights. These are then compared to previous estimates of ozone loss rates and discussed in the last section.

2 Measurements

For the first time ozone loss has been observed in situ over long periods of time by specially designed ultraviolet photometers (Kalnajs and Avallone, 2010) flown on long duration balloons launched as part of the Concordiasi campaign (Rabier et al., 2013) out of McMurdo Station, Antarctica in austral spring of 2010. These super-pressure balloons travel on constant density (isopycnic) surfaces; the 2010 Concordiasi payloads were launched to a density $\rho = 115$ g m⁻³ which corresponds to approximately 65 hPa (17 km). Of the nineteen balloons launched during Concordiasi, six (des-

ignated PSC-14 through 19) carried payloads with sensors to measure state parameters (T,p), ozone, and either particle size distribution via optical scattering or temperature profiles via GPS occultation. Ozone instruments were built by two groups - one at the Laboratoire de Météorologie Dynamique in Paris, France, hereafter referred to as LMDOz, and one at the University of Colorado Boulder, hereafter designated UCOz. Four of the six ozone balloons additionally carried laser particle counters from the University of Wyoming Ward et al. (2014).

The six payloads returned data every 15-30 minutes for periods ranging from 6 to 96 days; in all cases, the end of the data record was the result of communications failure with the payload rather than of instrument failure. By careful control of the balloon descent, three of the six payloads were unexpectedly recovered and the ozone sensors were returned to the laboratory for post-flight testing and calibration. In all cases, the post-flight diagnostics indicated that no degradation had taken place during flight and that the calibrations remained stable. Therefore, the ozone data discussed here are accurate to 20 ppb. The accuracy of the ozone instruments in flight was validated through coordinated ozonesonde launches from several Antarctic research stations. Ozone sondes were launched from each station when a PSC flight passed near the station; 12 comparisons between sonde and long duration ozone data were performed, with 5 concurrent comparisons having a separation of less than 100 km.

Data from three ozone instruments - those called PSC-14, PSC-16 and PSC-17 - are discussed in the analysis below. PSC-15 had a very short lifetime due to a battery failure on the balloon gondola. PSC-18 and PSC-19 were launched on 29 Sept and 8 Oct, respectively, after the majority of the ozone loss had taken place. Details of the three flights reported on here are given in Table 1.

3 Trajectories and match criteria

The balloon trajectories displayed in Figure 1 show that it takes approximately 10 days for the balloon to circumnavigate the Antarctic stratosphere. Figure 2 displays the ozone measurements and the corresponding potential temperature surfaces for the three trajectories shown in Figure 1. The balloons do not perfectly follow the air parcels. First, the Concordiasi balloons follow isopycnic (constant density) surfaces rather than constant potential temperature (isentropic) surfaces. Furthermore, the diurnal heating and cooling of the balloons produces clear diurnal variations in the potential temperatures. Care was therefore taken when matching the air-parcels to calculate the ozone loss. These variations were important because horizontal distances travelled between air-parcels of different potential temperature (even a few Kelvin apart) can be very large, due to the large wind shears and

velocities occurring in the stratospheric polar vortex - hence strict air-mass match criteria were applied.

Back-trajectories were generated using ATLAS (Wohltmann and Rex, 2008) driven by ERA-Interim meteorology and total radiative heating rates. The trajectories were initiated every 7.5 hours along the balloon flight path and calculated backwards until the balloon launch time. The trajectories were saved at 15 minute intervals. At each of the 15 minute intervals along the back trajectories the distance to the balloon at the corresponding time was calculated - this is termed the Match radius; other parameters such as PV and theta are also compared between the back-trajectory and the balloon location. Match pairs were defined following the definitions of Rex et al. (1999): each of the match pairs satisfying the following difference criteria: <1 K potential temperature, <1s⁻¹ potential vorticity and <10 days in time. The match radius (shortest distance between trajectory and balloon location) must be <300 km and the normalised potential vorticity (PV) along the entire trajectory must be < -36 s⁻¹ to ensure that the match occurs within the Antarctic polar vortex. The normalised PV is calculated using the following function:

$$PV_{Norm} = -0.265 \frac{PV}{PV_{Scale}} \quad (1)$$

$$PV_{Scale} = \frac{0.0981}{(b + 2c\theta + 3d\theta^2) \exp(\ln P)} \quad (2)$$

$$\ln P = a + b\theta + c\theta^2 + d\theta^4 \quad (3)$$

where θ is the potential temperature and the parameters $a=12.48$, $b=-3.212E-2$, $c=3.708E-5$, $d=-1.627E-8$ have been established from the relationship pressure, theta and PV from Antarctic ozonesonde matches.

To determine the ozone loss rate, a regression of the change in ozone versus sunlit hours or days for a number of matches was performed. After application of the match criteria, matches were binned according to the time period over which they sampled; i.e., when a match pair spanned days 264 to 272 it would be binned in the 255 - 265, 260 - 270 and 265 - 275 bins. More than 10 matches were required for a regression slope to be determined. As there was little potential temperature-dependence of the ozone loss rates (and theta varied maximally 20 K over the balloon lifetime), all matches were included, ignoring the potential temperature of the match. So while the potential temperature was important for determining the match, the resultant ozone loss rates were not sensitive to it.

JPL 2011 (Sander et al., 2011) chemistry was used to drive a chemical box model (Wohltmann and Rex, 2008) along one representative match trajectory for each 10 day period for each balloon. This provided an indication of the expected ozone loss rates assuming full chlorine activation ($ClO_x=Cl_y$). Br_y was 19.5-19.6 pptv for the simulations.

4 Results and Discussion

Analysis of the 2010 ozone hole by Klekociuk et al. (2011) shows it to be a one of the smallest in area since the discovery of the ozone hole. However, the total ozone loss in the lowermost stratosphere was seen to be similar to losses that occurred in previous recent years. Therefore the losses observed in 2010 can be seen as representative of perturbed springtime Antarctic ozone losses. Klekociuk et al. (2011) also found there was very little dynamical disturbance of the polar vortex after September; thus the rates observed by Concordiasi were not influenced by a premature break-up, in fact 2010 was one of the longest-lasting ozone holes on record, persisting into December.

Figure 3 and Figure 4 display the ozone loss rates per day per sunlit hour and day, respectively, determined by binning according to the longitude of the end match point. The four longitude quadrant bins are shown in the map insets (with their associated colours used in the line plot). Also displayed in black are box model calculated ozone loss rates using JPL 2011 kinetics and $ClO_x=Cl_y$, representing maximal expected loss rates. For the PSC-17 balloon the largest ozone loss rate was observed in the early time period for matches that ended in the 0 - 90°W quadrant (depicted in red) of Antarctica which has recently experienced the Antarctic Peninsula region. For PSC-16, the ozone loss rates were largest in the 90 - 180°W quadrant (depicted in yellow) which corresponds to the Ross Sea and Marie Byrd Land region for balloon PSC-16. The 0-90°E quadrant (blue) showed the largest losses in the later time periods. The ozone losses were very large for the earliest time period of 255-265 day of year (11th - 21st September). This is consistent with air-masses having PSC contact in the previous quadrants over East Antarctica (0-90°E). PSCs have been shown to have a higher incidence over the central and Antarctic Peninsula regions for altitudes between 15-20 km and are highly correlated with tropospheric systems that have clouds that reach above 7.5 km (Wang et al., 2008). The high ozone loss rates observed of 230 ppbv per day for PSC-17 are consistent with simulated loss rates using a box model (black line) which assumes complete chlorine activation. The loss rates observed for PSC-16 were significantly smaller than those simulated for complete chlorine activation, it is interesting to note that ozone loss rates of up to 380 ppbv per day would be possible when full activation is assumed ($ClO_x=2.7-2.9$ ppb). The box model calculated ozone loss rates for PSC-14 had a lower Cl_y of 2.3-2.4, compared to that used in the PSC-16 and PSC-17 calculations (ranging from 2.6-2.9 ppb - variations are due age of air). A higher Cl_y than used in the simulation of PSC-14 could explain why the calculated losses were smaller than those observed for the 260-270 day of year matches. As these box model calculations only represent a single match pair trajectory of the longest duration in each of the time periods, the box model simulated loss rates should be viewed as a guide only.

The balloon trajectories (Figures 1 and 3) show that the PSC-16 and PSC-17 balloons were largely displaced off the continent while in the 0-90°E and 0-90°W quadrants, respectively. As a result, these airmasses would have experienced larger exposures to sunlight at these northern latitudes. For PSC-16 this translated into higher ozone losses with match latitude (Figure 5, middle panel) but for PSC-17 the extreme ozone losses can not be attributed to more sunlight exposure (Figure 5, lower panel). For this balloon, the more negative mean PV values of the matches are associated with the large ozone losses (Figure 6). The PV displayed in Figure 6 are normalised thus more negative PV are associated with higher vorticities. Unfortunately, there are not sufficient statistics to determine this relationship for PSC-16. PSC-16 experienced the largest ozone losses when the match end point was in the 90-180°W sector (Ross sea and Marie Byrd Land), it was likely that the exposure to higher sunlight at northern latitudes that drove these losses and maintained the high ClO that was observed for PSC-16 over the days 260-270. Indeed the box model simulations show that chlorine activation is not complete for matches experienced by this balloon.

To understand the low sunlight exposure, yet very high ozone losses, for matches ending between days 255 and 265 seen by the PSC-17 balloon, examining the chlorine activation, as evidenced by the abundance of ClO (Figure 7), and PSC area (Figure 8) was necessary. The PSC-17 flight passed over the Antarctic Peninsula then stayed over the continent between days 255 and 265. The microwave limb sounder (MLS) onboard the Aura satellite ClO observations (Santee et al., 2008) at 68.13 hPa showed zonally symmetry for the 255 - 265 time period (figure 7, upper left panel), which is absent in the later time periods when the vortex was largely displaced toward the 0-90°E sector. The box model simulations show that the high observed PSC-17 ozone loss rates are consistent with full chlorine activation.

The PSC data from the CALIOP (Cloud-Aerosol Lidar with Orthogonal Polarization) onboard the CALIPSO (Cloud-Aerosol Lidar and Infrared Pathfinder Satellite Observations) satellite (Pitts et al., 2009) is shown in Figure 8. This shows that PSCs were present downwind of the Antarctic Peninsula region and largely absent from the Ross Sea region, 90-180°E and 90-180°W, respectively. So PSC-17 had maximum exposure to the Antarctic Peninsula PSC region and subsequently high ClO in the air-masses that it sampled. The resulting ozone losses of around 230 ppbv per day were seen for matches that had end points in the Antarctic Peninsula sector (i.e., airmasses have passed over the Peninsula mountains where large excursions of temperature and resulting PSC formation are known to take place), at latitudes poleward of 75°S and potential vorticities between -58 and -62 s⁻¹. This result is also consistent with the findings of Kohma and Sato (2013) who attribute a 20% probability of PSC formation due to anticyclonic clouds in the troposphere for September (it is higher for the winter months). The Antarctic Peninsula, but also Marie Byrd Land, are cited

as important geographical regions for PSC formation.

Table 2 compares the ozone loss rates calculated here with those found previously in the literature for the Antarctic region. The vortex-average values from Concordiasi are in good agreement with the ozonesonde match campaign held in 2003 and satellite estimates from POAM III and Sciamachy. Comparisons with ozone losses determined from sondes launched at a single station also show consistency. However, what is hidden in the vortex-average is how fast the ozone loss can be over the geographic region of the Antarctic Peninsula when conditions are favourable. Losses of up to 230 ppbv per day are exceptional and dictate the speed at which the ozone hole forms in early September. However, box model simulations suggest that even higher rates of up to 380 ppbv per day could be possible if full chlorine activation was achieved.

5 Conclusions

Ozone loss rates were derived from the Concordiasi quasi-Lagrangian long duration balloons flown at 17km (65 hPa) over Antarctica in September of 2010, which carried instrumentation that measured ozone continuously in-situ for the first time. The loss rates were similar to previously reported Antarctic vortex-average loss rates of 6±6 ppbv per sunlit hour or 74 ±70 ppbv per day. However, exceptionally rapid ozone loss rates of 230 ppbv per day (20 ppbv per sunlit hour) were observed for airmasses that traversed the Antarctic Peninsula region while remaining at high latitudes and high absolute PV. This geographical maximum in the ozone loss rates is consistent with high PSC occurrence and large ClO abundances present during September (12th-22nd) as observed from Calipso and MLS, respectively, downstream of the Antarctic Peninsula region. Box model simulations show this large ozone loss rate is consistent with full chlorine activation.

Previous Antarctic ozone loss rates have considered vortex-average losses exclusively. By moving away from this view, these high fidelity Concordiasi ozone observations and derived ozone loss rates downstream of the Antarctic Peninsula can be used to test the ability of chemistry climate models to capture the timing and spatial variations of ozone hole formation. A comparison of these loss rates and chemical transport simulations using laboratory based reaction rates is beyond the scope of this paper, and makes up a future study that explores the chlorine dimer kinetics and their uncertainties.

These high fidelity ozone measurements onboard long duration balloon flights have provided valuable spatial insight into Antarctic polar ozone loss. The upcoming Strateole 2 experiment will be instrumented with ozone sensors such as those used in Concordiasi, providing the potential for in situ insights into tropical ozone chemistry in the lowermost stratosphere. This is a region where satellite retrievals are

challenged and questions concerning the ozone loss rates on cold stratospheric aerosol could potentially be addressed.

Acknowledgements. Concordiasi is an international project, currently supported by the following agencies: Mto-France, CNES, 385 CNRS/INSU, NSF, NCAR, University of Wyoming, Purdue University, University of Colorado, the Alfred Wegener Institute, the Met Office, and ECMWF. Concordiasi also benefits from logistic or financial support of the operational polar agencies Institut Polaire Franais Paul Emile Victor (IPEV), Programma Nazionale di 390 Ricerche in Antartide (PNRA), United States Antarctic Program (USAP) and British Antarctic Survey (BAS), and from Baseline Surface Radiation Network (BSRN) measurements at Concordia. Concordiasi is part of The Observing System Research and Predictability Experiment-International Polar Year (THORPEX-IPY) 400 cluster within the International Polar Year effort. The Concordiasi website can be found at www.cnrm.meteo.fr/concordiasi/. The PSC mask data from the Calipso instrument were obtained from the NASA Langley Research Center Atmospheric Science Data Center. The Microwave Limb Sounder CIO data were obtained 405 from Nathaniel Livesey. The authors thank ECMWF for providing ERA-Interim data via special project DERESI. RS received funding support for this work from the European Union (EU) WaVES (MIF1-CT-2006-039646) project, Australian Antarctic Science Grant (FoRCES 4012) and the Australian Research Councils 410 Centre of Excellence (CE110001028) scheme. LMA and LEK acknowledge support from the US National Science Foundation under grant ANT-0839017. 415

References

- Bekki, S., Bodeker, G., Bais, A. F., Butchart, N., Eyring, V., Fahney, D., Kinnison, D. E., Langematz, U., Mayer, B., Portmann, R., Rozanov, A., Braesicke, P., Charlton-Perez, A. J., Chubarova, N. E., Cionni, I., Diaz, S. B., Gillett, R., Giorgetta, M. A., Komala, N., Lefevre, F., McLandress, C., Perlwitz, J., Peter, T., and Shibata, K.: Future Ozone and Its Impact on Surface UV, in: Scientific Assessment of Ozone Depletion: 2010, Global Ozone 415 Research and Monitoring Project - Report No. 52, p. 516 pp., World Meteorological Organization, Geneva, Switzerland, 2011.
- Bevilacqua, R. M., Aellig, C. P., Debrestian, D., Fromm, M., Hoppel, K., Lumpe, J., Shettle, E., Hornstein, J., Randall, C., Rusch, D., and Rosenfield, J. E.: POAM II ozone observations in the 420 Antarctic ozone hole in 1994, 1995, and 1996, *Journal of Geophysical Research*, 102, 23 643–23 657, 1997.
- Dameris, M., Godin-Beekman, S., Alexander, S. P., Braesicke, P., Chipperfield, M., de Laat, A. T. J., Orsolini, Y., Rex, M., and Santee, M. L.: Update on Polar Ozone: Past, Present, and Future, 425 in: Scientific Assessment of Ozone Depletion: 2014, pp. 1–67, Global Ozone Reserach and Monitoring Project - Report No. 55, World Meteorological Organization, Geneva, Switzerland, 2014.
- Frieler, K., Rex, M., Salawitch, R. J., Canty, T., Streibel, M., Stimpfle, R. M., Pfeilsticker, K., Dorf, M., Weisenstein, D. K., 430 and Godin-Beekmann, S.: Toward a better quantitative understanding of polar stratospheric ozone loss, *Geophys. Res. Lett.*, 33, 2006.
- Hassler, B., Daniel, J. S., Johnson, B. J., Solomon, S., and Oltmans, S.: An assessment of changing ozone loss rates at South Pole: 435
- Twenty-five years of ozonesonde measurements, *Journal of Geophysical Research*, 116, 2011.
- Hoppel, K., Bevilacqua, R., Canty, T., Salawitch, R., and Santee, M.: A measurement/model comparison of ozone photochemical loss in the Antarctic ozone hole using Polar Ozone and Aerosol Measurement observations and the Match technique, *Journal of Geophysical Research*, 110, –, 2005.
- Kalnajs, L. E. and Avallone, L. M.: A Novel Lightweight Low-Power Dual-Beam Ozone Photometer Utilizing Solid-State Optoelectronics, *Journal of Atmospheric and Oceanic Technology*, 27, 869–880, 2010.
- Klekociuk, A. R., Tully, M. B., Alexander, S. P., Dargaville, R. J., Deschamps, L. L., Fraser, P. J., Gies, H. P., Henderson, S. I., Javorniczky, J., KRUMMEL, P. B., Petelina, S. V., Shanklin, J. D., Siddaway, J. M., and Stone, K. A.: The Antarctic ozone hole during 2010, *Australian Meteorological and Oceanographic Journal*, 61, 253–267, 2011.
- Kohma, M. and Sato, K.: Simultaneous occurrence of polar stratospheric clouds and upper-tropospheric clouds caused by blocking anticyclones in the Southern Hemisphere, *Atmos Chem Phys*, 13, 3849–3864, 2013.
- Molina, L. and Molina, M.: Production of ClO₂ From the Self-Reaction of the ClO Radical, *J Phys Chem*, 91, 433–436, 1987.
- Pitts, M. C., Poole, L. R., and Thomason, L. W.: CALIPSO polar stratospheric cloud observations: second-generation detection algorithm and composition discrimination, *Atmospheric Chemistry and Physics*, 9, 7577–7589, 2009.
- Rabier, F., Cohn, S., Cocquerez, P., Hertzog, A., Avallone, L., Deshler, T., Haase, J., Hock, T., Doerenbecher, A., Wang, J., Guidard, V., Thépaut, J.-N., Langland, R., Tangborn, A., Balsamo, G., Brun, E., Parsons, D., Bordereau, J., Cardinali, C., Danis, F., Escarnot, J.-P., Fourrié, N., Gelaro, R., Genthon, C., Ide, K., Kalnajs, L., Martin, C., Meunier, L.-F., Nicot, J.-M., Perttula, T., Potts, N., Ragazzo, P., Richardson, D., Sosa-Sesma, S., and Vargas, A.: The Concordiasi Field Experiment over Antarctica: First Results from Innovative Atmospheric Measurements, *Bull. Amer. Met. Soc.*, 94, ES17–ES20, 2013.
- Rex, M., von der Gathen, P., Harris, N., Lucic, D., Knudsen, B. M., Braathen, G., Reid, S., de Backer, H., Claude, H., and Fabian, R.: In situ measurements of stratospheric ozone depletion rates in the Arctic winter 1991/1992: A Lagrangian approach, *Journal of Geophysical Research*, 103, 5843–5853, 1998.
- Rex, M., von der Gathen, P., Braathen, G., Harris, N., Reimer, E., Beck, A., Alfier, R., Kruger-Carstensen, R., Chipperfield, M., de Backer, H., Balis, D., O'Connor, F., Dier, H., Dorokhov, V., Fast, H., Gamma, A., GIL, M., Kyro, E., Litynska, Z., Mikkelsen, S., Molyneux, M., Murphy, G., Reid, S., Rummukainen, M., and Zerefos, C.: Chemical ozone loss in the Arctic winter 1994/95 as determined by the Match technique, *Journal of Atmospheric Chemistry*, 32, 35–59, 1999.
- Rex, M., Salawitch, R., Harris, N., von der Gathen, P., Braathen, G., Schulz, A., Deckelmann, H., Chipperfield, M., Sinnhuber, B., Reimer, E., Alfier, R., Bevilacqua, R., Hoppel, K., Fromm, M., Lumpe, J., Kullmann, H., Kleinbohl, A., Bremer, H., von Konig, M., Kunzi, K., Toohey, D., Vömel, H., Richard, E., Aikin, K., Jost, H., Greenblatt, J., Loewenstein, M., Podolske, J., Webster, C., Flesch, G., Scott, D., Herman, R., Elkins, J., Ray, E., Moore, F., Hurst, D., Romashkin, P., Toon, G., Sen, B., Margitan, J., Wennberg, P., Neuber, R., Allart, M., Bojkov, B., Claude,

- 495 H., Davies, J., Davies, W., de Backer, H., Dier, H., Dorokhov,
V., Fast, H., Kondo, Y., Kyro, E., Litynska, Z., MIKKELSEN,
I., Molyneux, M., Moran, E., Nagai, T., Nakane, H., Parrondo,
C., Ravegnani, F., Skrivankova, P., Viatte, P., and Yushkov, V.:
500 Chemical depletion of Arctic ozone in winter 1999/2000, *Journal of Geophysical Research*, 107, doi:10.1029-2001JD000 533,
2002.
- Sander, S. P., Friedl, R., Golden, D., Kurylo, M. J., Wine, P. H.,
Abbatt, J., Burkholder, J. B., Kolb, C. E., Moortgat, G. K., Huie,
R. E., and Orkin, V. L.: Chemical Kinetics and Photochemical
505 Data for Use in Atmospheric Studies - Evaluation No. 17, JPL
Publication 10-6, pp. 1-684, 2011.
- Santee, M. L., Lambert, A., Read, W. G., Livesey, N. J., Manney,
G. L., Cofield, R. E., Cuddy, D. T., Daffer, W. H., Drouin, B. J.,
Froidevaux, L., Fuller, R. A., Jarnot, R. F., Knosp, B. W., Pe-
510 run, V. S., Snyder, W. V., Stek, P. C., Thurstans, R. P., Wagner,
P. A., Waters, J., Connor, B., Urban, J., Murtagh, D., Ricaud, P.,
Barret, B., Kleinboehl, A., Kuttippurath, J., Kuellmann, H., von
Hobe, M., Toon, G. C., and Stachnik, R. A.: Validation of the
Aura Microwave Limb Sounder ClO measurements, *Journal of*
515 *Geophysical Research*, 113, doi:10.1029-2007JD008 762, 2008.
- Solomon, S.: Stratospheric ozone depletion: A review of concepts
and history, *Reviews of Geophysics*, 37, 275-316, 1999.
- Sonkaew, T., von Savigny, C., Eichmann, K. U., Weber, M.,
Rozanov, A., Bovensmann, H., Burrows, J. P., and Groöß,
520 J. U.: Chemical ozone losses in Arctic and Antarctic polar win-
ter/spring season derived from SCIAMACHY limb measure-
ments 2002-2009., *Atmos Chem Phys*, 13, 2013.
- Thompson, D. W. and Solomon, S.: Interpretation of recent South-
ern Hemisphere climate change, *Science*, 296, 895-899, 2002.
- 525 Thompson, D. W. J., Solomon, S., Kushner, P. J., England, M. H.,
Grise, K. M., and Karoly, D. J.: Signatures of the Antarctic
ozone hole in Southern Hemisphere surface climate change, *Nature*
Geoscience, 4, 741-749, 2011.
- von der Gathen, P., Rex, M., Harris, N. R. P., Lucic, D., Knudsen,
530 B. M., Braathen, G. O., De Backer, H., Fabian, R., Fast, H., Gil,
M., Kyrö, E., Mikkelsen, I. S., Rummukainen, M., Stähelin, J.,
and Varotsos, C.: Observational evidence for chemical ozone de-
pletion over the Arctic in winter 1991/92, *Nature*, 375, 131-134,
1995.
- 535 Wang, Z., Stephens, G., Deshler, T., Trepte, C., Parish, T., Vane, D.,
Winker, D., Liu, D., and Adhikari, L.: Association of Antarctic
polar stratospheric cloud formation on tropospheric cloud sys-
tems, *Geophysical Research Letters*, 35, L13 806, 2008.
- Ward, S. M., Deshler, T., and Hertzog, A.: Quasi-Lagrangian mea-
540 surements of nitric acid trihydrate formation over Antarctica,
Journal of Geophysical Research-Atmospheres, 119, 245-258,
2014.
- Wohlmann, I. and Rex, M.: Improvement of vertical and resid-
545 ual velocities in pressure or hybrid sigma-pressure coordinates
in analysis data in the stratosphere, *Atmospheric Chemistry and*
Physics, 8, 265-272, 2008.

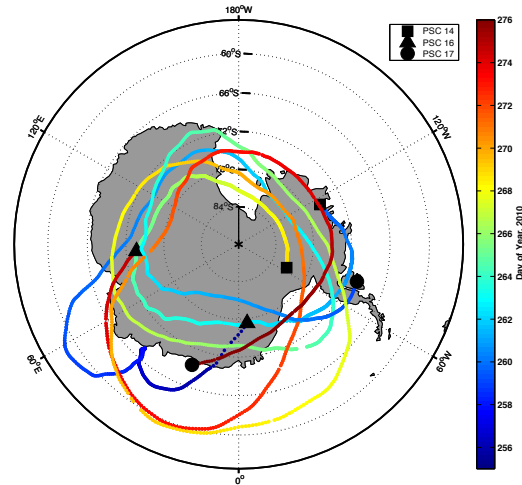


Fig. 1. The flight paths of the three ozone Concordiasi balloons are displayed.

Table 1. Details of balloon flights analysed for ozone loss rates

	PSC-14	PSC-16	PSC-17
Instrument	LMDOz	UCOz	UCOz
Launch date	5 Sept 0310 UT	11 Sept 0300 UT	14 Sept 0150 UT
Last data record	21 Dec 1428 UT	4 Oct	15 Oct
Distance travelled (km)	147,500	34,565	59,034
Days used to calculate ozone loss rates	259 - 269 16 - 23 Sept	255 - 275 12 Sept - 2 Oct	259 - 277 16 Sept - 4 Oct
Theta range (K)	404-425	416-437	414-436
Pressure range (hPa)	62-66	62-69	64-69

Table 2. Comparison of Antarctic stratospheric ozone loss rates

Method	Time	Area	Ozone Loss Rate (ppbv day ⁻¹) (ppbv sunlit hr ⁻¹)	Reference
Concordiasi (410-430 K)	12 - 22 Sept: 2010	vortex-average	74 ± 70 6 ± 6	This work
POAM II (500 K)	1 - 30 Sept: 1994, 1995, 1996	vortex-average	85 ± 15	(Bevilacqua et al., 1997, Figure 9)
POAM III (445-523 K)	1 - 15 Sept: 1998-2003	vortex-average	8 ± 6	(Hoppel et al., 2005, Figure 9)
Ozonesondes (500 K)	15 Aug - 15 Sept: 2003	vortex-average	4 ± 1	(Frierler et al., 2006, Figure 1)
Ozonesondes (475-500 K)	23 Aug - 27 Sept: 1991-1995 1996-2010	89.98°S	90 ± 10 70 ± 10	(Hassler et al., 2011, Figure 5)
SCIAMACHY (475 K)	18 Aug - 18 Sept: 2002 - 2008	vortex-average	45 ± 6	Sonkaew et al. (2013)
Average	1991 - 1995 1996 - 2010		88 ± 18 54 ± 16	

Uncertainties given as 1 standard deviation.

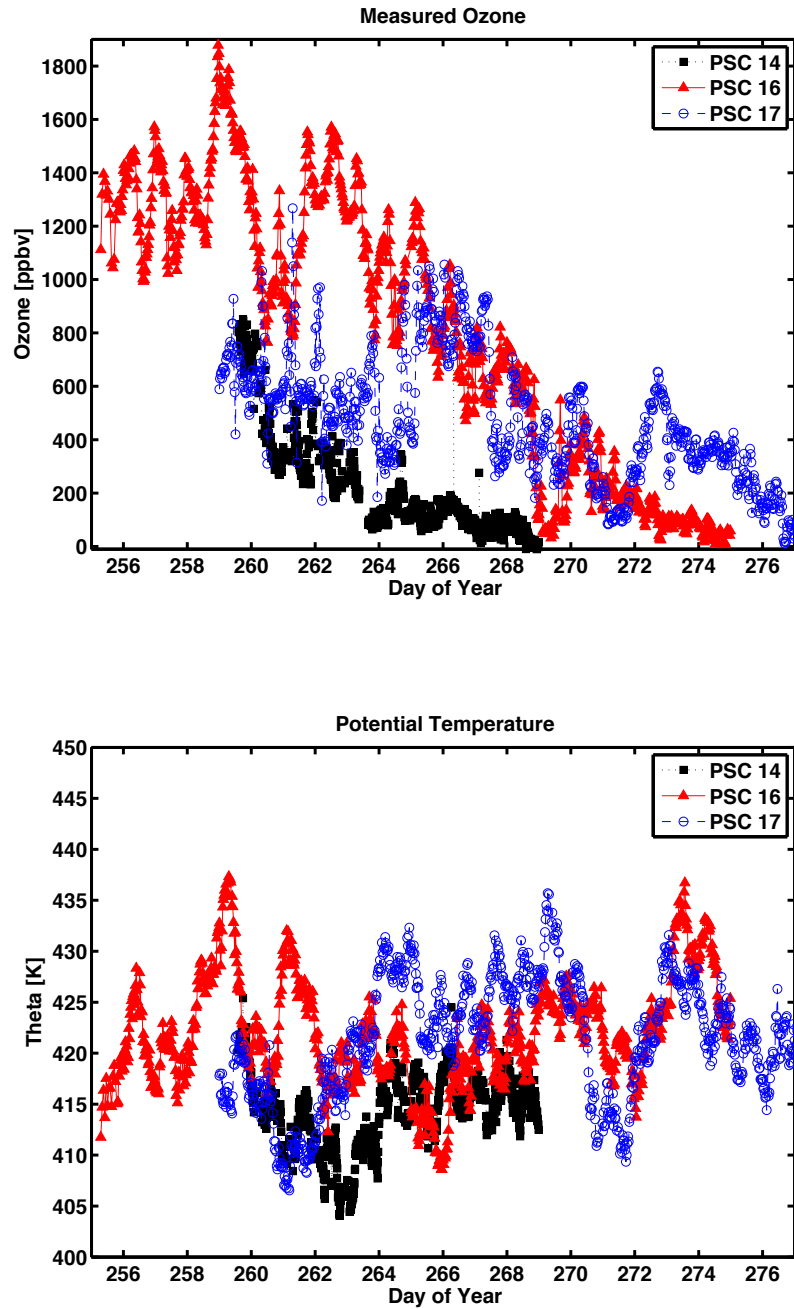


Fig. 2. Ozone and potential temperature along the trajectory of each of the ozone instrumented Concordiasi balloons. Clearly measured is the ozone loss under perturbed springtime conditions. The diurnal heating and cooling of the balloon is evident in the potential temperature variations.

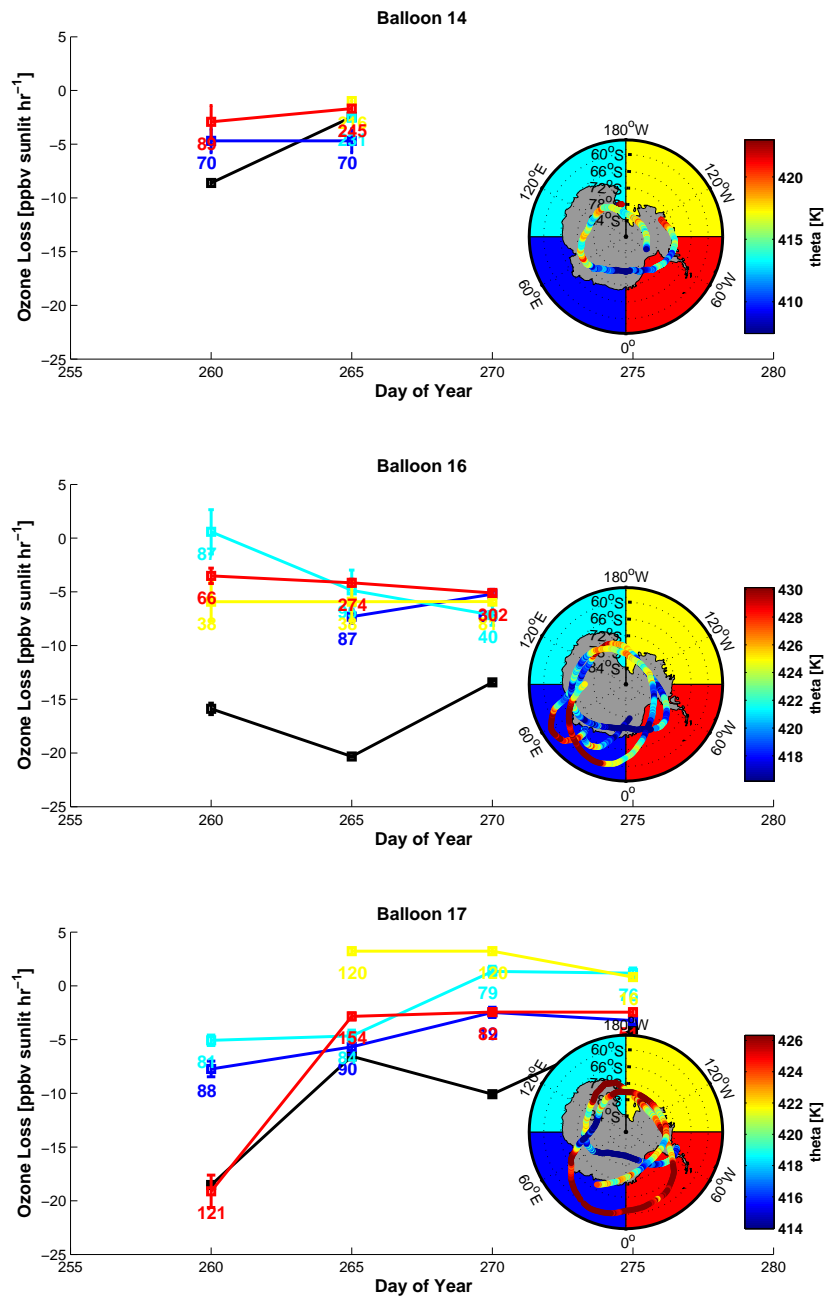


Fig. 3. Ozone loss per sunlit hour for all of the matches for each of the ozone instrumented Concordiasi balloon flights. The matches are binned into the longitude quadrant of their end match (blue: 0-90°E, turquoise: 90-180°E, yellow 90-180°W and red 0-90°W). While each match requires the potential temperature to be within 1K, all matches with an initial or end match within ± 5 days are binned to give the ozone versus sunlit hour regression shown. This way a match ending on day 263 will be represented in both the 260 and 265 data points above. The colour bar is used to indicate the potential temperature of the ozone observations as plotted with dots on the map. The error bars represent the standard error of each regression fit, and the coloured numbers the number of matches used in the regression fitting. Also shown is simulated ozone loss rates calculated by running a chemical box model along the longest match trajectory for each time bin (black line). The box model assumes $\text{ClO}_x = \text{Cl}_y$ and JPL 2011 kinetics.

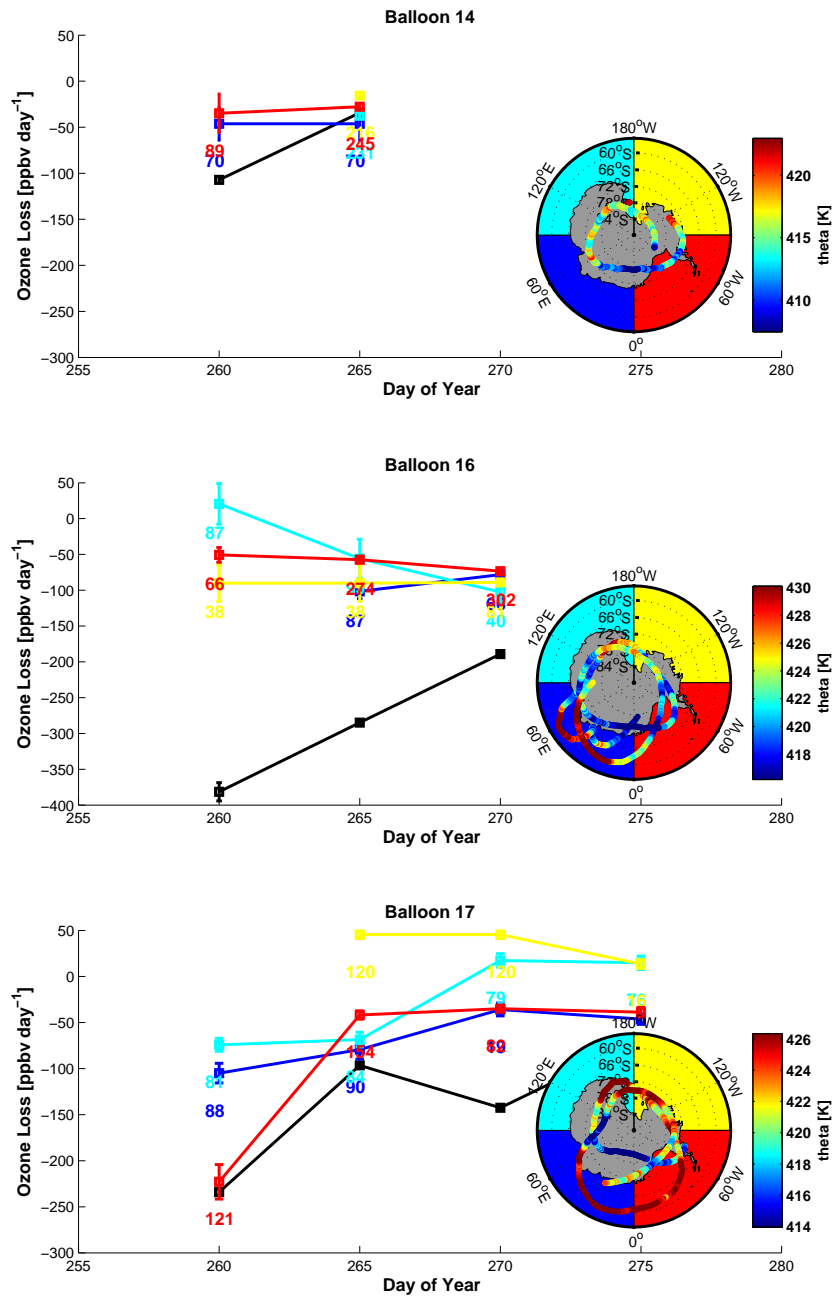


Fig. 4. As figure 3 but for ozone loss per day.

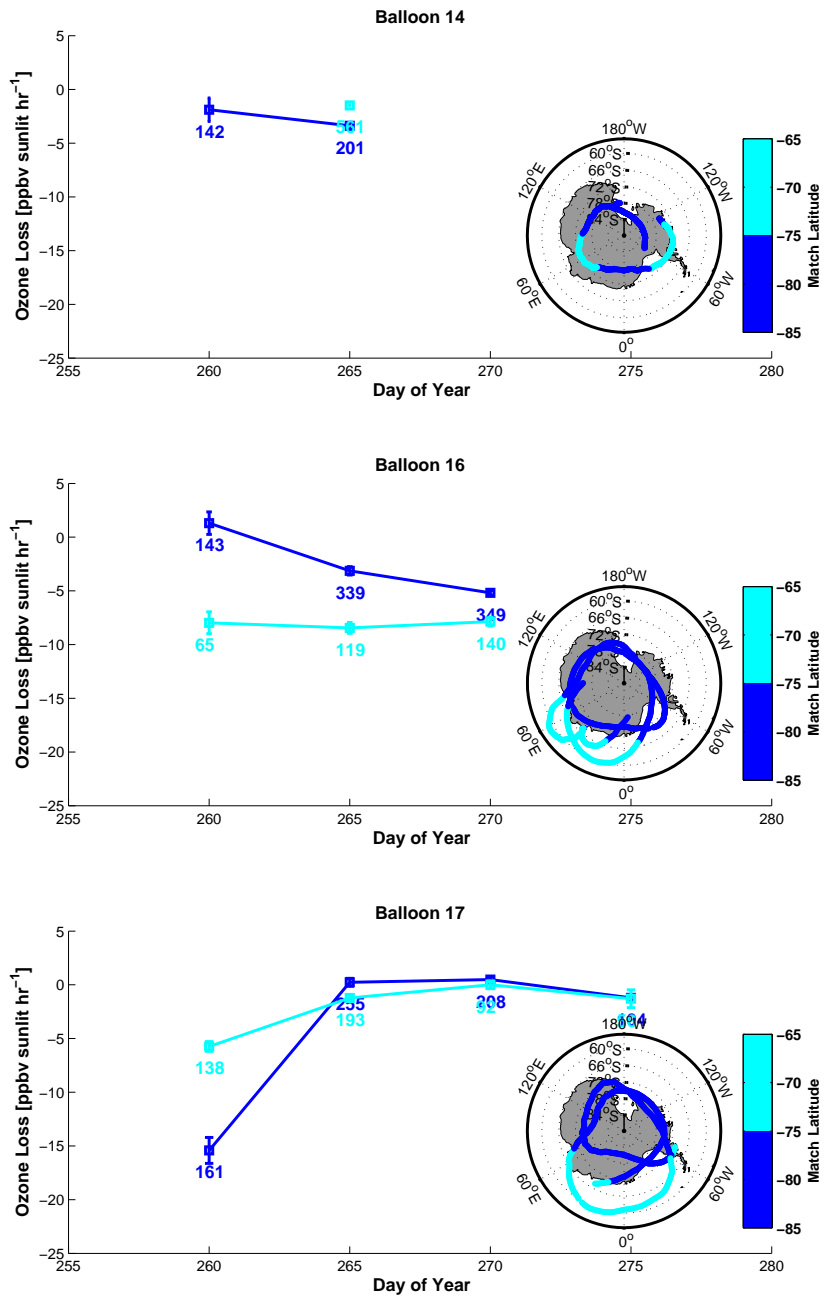


Fig. 5. Ozone losses binned according to mean latitude of the match.

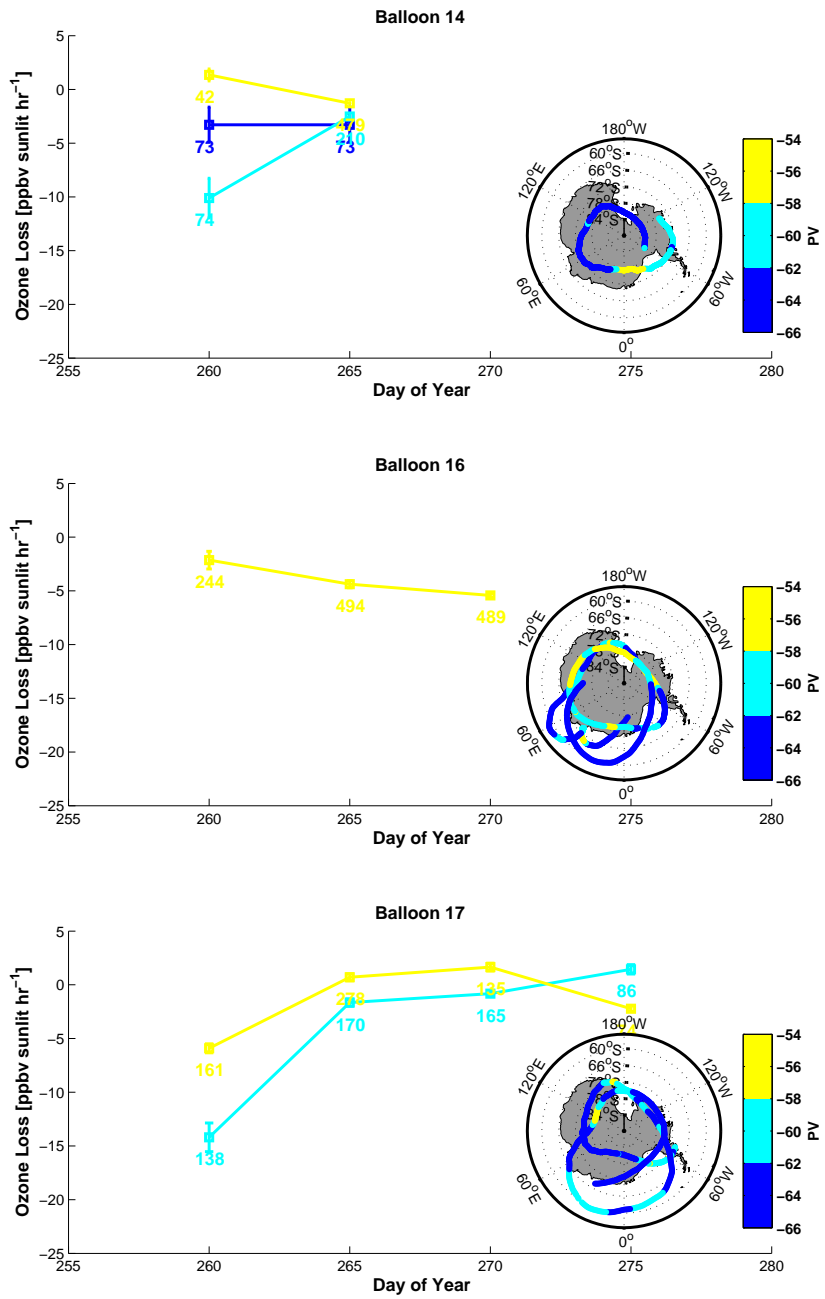


Fig. 6. Ozone loss according to mean normalised PV of the match.

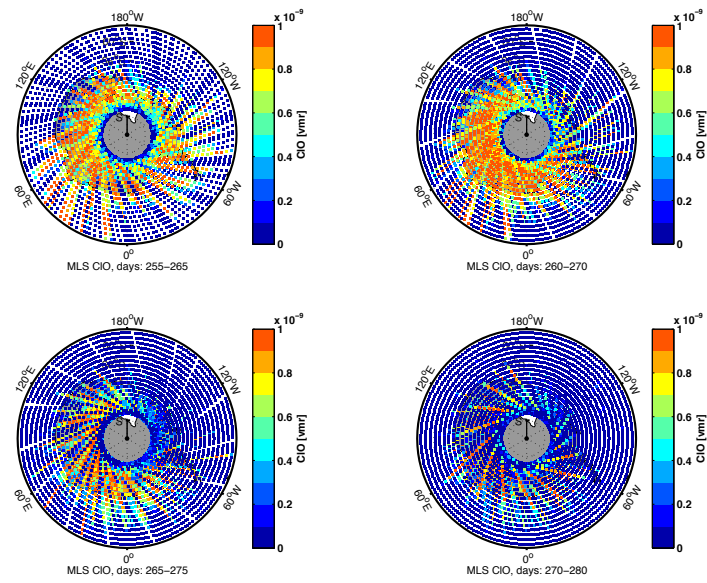


Fig. 7. Microwave Limb Sounder ClO data retrieved on the 68.13 hPa level over the ten day periods used for the four ozone loss calculations in Figures 3 and 4.

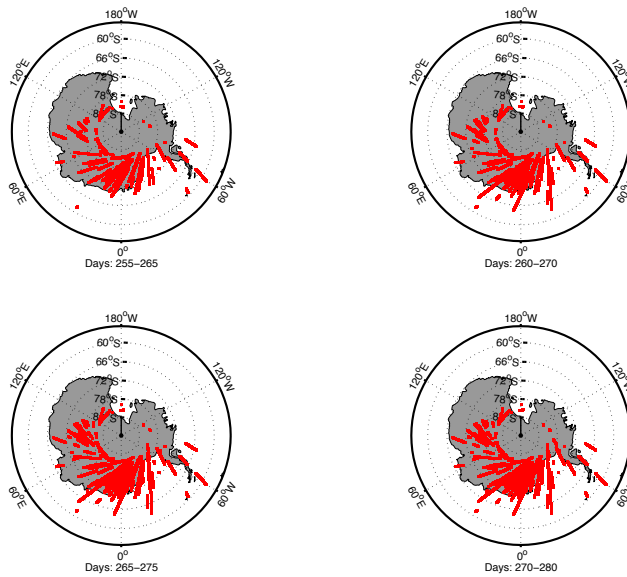


Fig. 8. Calipso PSC flag over the 10 day bin intervals used in the ozone loss calculations for the 16.7 km altitude layer.